HHS Public Access

Author manuscript

Synapse. Author manuscript; available in PMC 2024 September 01.

Published in final edited form as:

Synapse. 2023 September ; 77(5): e22279. doi:10.1002/syn.22279.

Relationships of *in vivo* brain norepinephrine transporter and age, BMI, and gender

Sheida Koohsari[1], **Faranak Ebrahimian Sadabad**[1], **Brian Pittman**[2], **Jean-Dominque Gallezot**[1], **Richard E. Carson**[1], **Christopher H. van Dyck**[2], **Chiang-shan R. Li**[2], **Marc N. Potenza**[2,3,4,5,6,7], **David Matuskey**[1,2,8]

[1]Department of Radiology and Biomedical Imaging, Yale University, New Haven, CT

[2]Department of Psychiatry, Yale School of Medicine, New Haven, CT

[3]Child Study Center, Yale School of Medicine, New Haven, CT

[4]Department of Neuroscience, Yale University, New Haven, CT

[5]Connecticut Council on Problem Gambling, Wethersfield, CT

[6]Connecticut Mental Health Center, New Haven, CT

[7]Wu Tsai Institute, Yale University, New Haven, CT

[8]Department of Neurology, Yale University, New Haven, CT

Abstract

Objective: Previous research reported an age-related decline in brain norepinephrine transporter (NET) using (S,S)-[11C]O-methylreboxetine ([11C]MRB) as a radiotracer. Studies with the same tracer have been mixed in regards to differences related to body mass index (BMI). Here, we investigated potential age-, BMI-, and gender-related differences in brain NET availability using [11C]MRB, the most selective available radiotracer.

Method: Forty-three healthy participants (20 females, 23 males; age range 18-49 years), including 12 individuals with normal/lean weight, 15 with overweight, and 16 with obesity were scanned with [11C]MRB using a positron emission tomography (PET) high-resolution research tomograph (HRRT). We evaluated binding potential (BP_{ND}) in brain regions with high NET availability using multilinear reference tissue model 2 (MRTM2) with the occipital cortex as a reference region. Brain regions were delineated with a defined anatomic template applied to subjects' structural MR scans.

Result: We found a negative association between age and NET availability in the locus coeruleus, raphe nucleus, and hypothalamus, with a 17%, 19%, and 14% decrease per decade, respectively, in each region. No gender or BMI relationships with NET availability were observed.

Conclusion: Our findings suggest an age-related decline, but no BMI- or gender-related differences, in NET availability in healthy adults.

Data Availability Statement: The authors confirm that the data supporting the findings of this study are available within the article and its supplementary materials.

Graphical Abstract

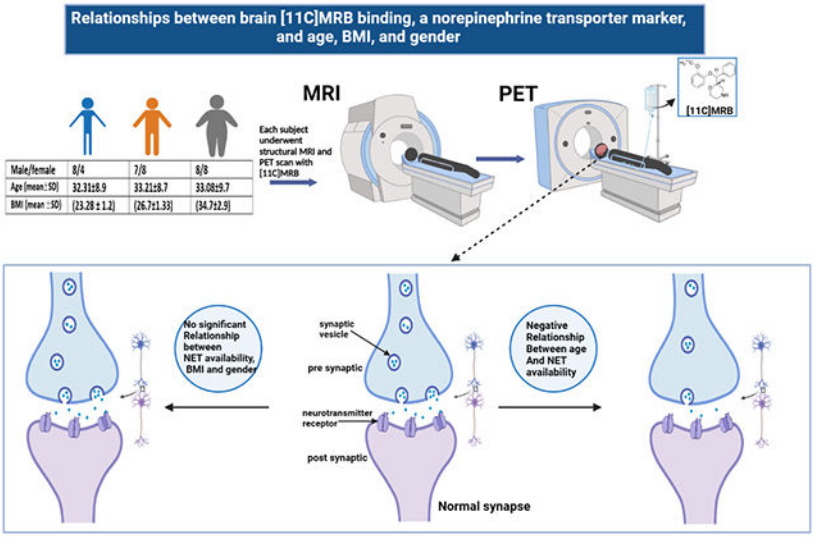

Keywords

MRB; NET; norepinephrine transporter

Introduction

The norepinephrine transporter (NET) is a transmembrane protein that is the principal regulator in norepinephrine (NE) synapses. There is evidence of NET involvement in various neuropsychiatric conditions, such as Parkinson's disease (McMillan et al., 2011), Alzheimer's disease (Szot et al., 2000), epilepsy (Kaminski et al., 2005), depression (Klimek et al., 1997), attention deficit hyperactivity disorder (ADHD) (Sigurdardottir et al., 2021), stress-related disorders (Miner et al., 2006), and psychostimulant abuse (Weinshenker and Schroeder, 2007).

Given the importance of NET in neuropsychiatric conditions, positron emission tomography (PET) has the opportunity to quantify *in vivo* NET availability in the brain and may offer important insight into conditions with reduced NET availability like ADHD (Ulke et al,2019) or increased availability such as patients with major depressive disorder (Moriguchi et al, 2017). Among available radioligands, (S, S)-[11C] O methylreboxetine ([11C]MRB) has shown the most promise for studying brain NET distribution and may provide insight into other important individual differences (Ding et al., 2005; Ding et al., 2006).

While NE is a vital neurotransmitter with wide distribution in the brain, the locus coeruleus (LC) is recognized as the substantial producer of NE (Lorang et al., 1994) with projections to other areas. Several histopathologic studies have revealed decreases in the number of LC neurons in the brain with aging (Manaye et al., 1995; Chan-Palay and Asan, 1989; Vijayashankar and Brody, 1979). Likewise, an [11C]MRB PET study in cocaine use disorder showed decreased binding potential (BP_{ND}) with aging in a limited number of control participants (N=12) in the LC, pulvinar, and hypothalamus (Ding et al., 2010).

NE has been implicated in disorders with gender-related differences, like depression and anxiety. Thus, considering gender in NET studies is important. Preclinical studies have reported sex hormones' influences on brain NET expression and hypothesized that gonadal hormones affect NE activity, and in response, NE is involved in gonadal steroid feedback on secretion of luteinizing hormone (Shang and Dluzen, 2002; Yang et al., 1997). To our knowledge, however, this is the first study investigating whether gender-related differences in NET availability exist in the human brain *in vivo*.

Likewise, relationships between NET and body mass index (BMI) have attracted attention, in part due to NE and dopamine involvement in feeding behavior and biology. Several PET studies have examined BMI in brain NET using [11C]MRB. One of these conducted at Yale found between group differences between obese and normal/lean weight individuals in the thalamus, but not in other regions (Li et al., 2014). Another study with the same tracer performed by Hesse and colleagues did not find significant differences people with and without obesity (Bresch et al., 2017a, Hesse et al., 2017). Interestingly, the same group found within-obesity-group relationships with [11C]MRB BP_{ND} values suggestive of NET involvement in eating behaviors like emotional eating and susceptibility to hunger (Bresch et al., 2017b; Bresch et al., 2017a). They also suggested that NET availability might be helpful as a biomarker for predicting outcomes to dietary interventions, which could inform individualized treatment of obesity (Vettermann et al., 2018).

In the present study, we investigated the relationships between age, gender, and BMI and brain NET binding in healthy individuals using [11C]MRB.

Methods:

Subjects:

PET data of forty-three healthy subjects (20 female, 23 male; age range 18-49 years), including 12 with normal/lean BMI, 15 with overweight, and 16 with obesity, with mean BMI scores of 23.28 ± 1.2; 26.7±1.3 and 34.7±2.9 respectively. Gender distribution in each BMI group was 4 females and 8 males in the normal weight group, 8 females and 7 males in the overweight group and 8 females and 8 males in the obese group (Supplementary table 2). Subjects were obtained from unpublished and previous studies (Li et al., 2014; Hannestad et al., 2010). All participants underwent a comprehensive medical assessment and were free of present or past major medical illnesses, including significant neurological and psychiatric disorders. Subjects reported no history of substance use, had negative urine toxicology tests at the time of the PET scan and had no contraindications for MRI scans. The study was administered under protocols approved by the Yale Human Investigation Committee, the Yale University Radiation Safety Committee, and the Yale MRI Safety Committee. All participants signed an informed consent after a thorough explanation of the study procedures.

PET Imaging:

[11C]MRB was prepared as previously described (Ding et al., 2003). Subjects underwent 120 minutes of emission scanning using a High-Resolution Research Tomograph (HRRT)

scanner (207 slices, resolution 2.5 mm FWHM in 3D acquisition mode). For attenuation correction, transmission scans with an orbiting 137Cs point source were acquired before radiotracer injection. For each subject, a bolus dose of 596±150 (mean ± SD) MBq [11C]MRB was injected through a venous catheter in 2 minutes. Measurements from the Vicra (NDI systems, Waterloo, Canada), a motion-tracking tool, were used for motion correction. PET imaging was performed in list mode with the time frame of 6 × 30 s; 3 × 1min; 2 × 2min, 22 × 5 min. Dynamic images were reconstructed using ordered subset expectation maximization (OSEM, 2 iterations, and 30 subsets) and corrected for attenuation, normalization, scatter, random events, dead time, and event-by-event motion using the Motion-compensation OSEM List-mode Algorithm for Resolution-recovery Reconstruction (MOLAR) algorithm, as previously described (Carson et al., 2003).

MRI imaging:

Structural T1-weighted MRI imaging was performed on a Siemens 3-Tesla scanner (Trio or Prisma; Siemens AG, Erlangen, Germany) with a circularly polarized head coil for anatomical co-registration with PET imaging. The 3-dimensional acquisition parameters were 256 · 256 · 176, and the voxel size of the MR image was 0.98 · 0.98 · 1.0 mm.

Image analyses:

A summed PET image (0–10 min after injection) was coregistered to the subject's MRI, then linearly registered to an MRI template to identify regions of interest (ROIs) based on the Automated Anatomical Labeling template (AAL) (Tzourio-Mazoyer et al., 2002). Brain regions were incorporated into the template after being hand-drawn on the generated average PET image (Ding et al., 2010). A normalized mutual information algorithm was used for the transformation (FLIRT, http://www.fmrib.ox.ac.uk/analysis/research/flirt). Regional nondisplaceable binding potential (BP_{ND}) was quantified using the occipital cortex as a reference region as has been previously done. No effects were seen in the reference region in relation to age or BMI (Hannestad et al., 2010). The multilinear reference tissue model 2 (MRTM2; Ichise et al., 2003) was applied for parametric images of binding potential. Areas with the highest BP_{ND} values were included: LC, pulvinar, raphe nucleus, red nucleus, thalamus, and hypothalamus.

Statistical analysis:

NET availability levels were assessed for normality prior to analysis using normal probability plots and the Kolmogorov test statistics. The outcome was approximately normal. A linear mixed model was utilized to investigate the association between BP_{ND} values and age, gender, and BMI. As the injection dose (596±150 MBq) was significant in regards to the primary outcomes ($F(1,38)= 4.8$, $p=0.03$), we used it as a covariate in all mixed model analyses. To account for within-subject correlations, three variance-covariance structures were fit to the data (unstructured, compound symmetry, and heterogeneous compound symmetry). According to the Bayesian information criterion (BIC), an unstructured variance-covariance fit the data best. All analyses were conducted using SAS, version 9.1 (SAS Institute Inc.). Potential associations between BP_{ND} values and age, gender and BMI were estimated using Pearson correlations.

Results

A significant region by age interaction was observed ($F(5, 38) = 2.55$, $p = 0.044$). Mean levels of [11C]MRB BP_{ND} values for all regions, slopes estimated from the model, and correlations with age are reported in Table 1. A statistically significant negative association was observed between age and NET availability in the hypothalamus ($t(38) = -2.49$, $p = 0.0174$), LC ($t(38) = -3.02$, $p = 0.0045$), and raphe nucleus ($t(38) = -3.85$, $p = 0.0004$) (Supplementary fig. 1). The average decline per decade is shown in Table 1, and Figure 1 shows age relationships with LC BP_{ND} values. BMI demonstrated no significant relationship with NET availability in any brain region. Likewise, there were no significant differences between males and females in NET availability. For detailed information, see the supplementary data.

Discussion

To our knowledge, this is the largest sample to date measuring NET in the brain of healthy individuals. Aligned with a previous study (Ding et al., 2010), lower NET availability was seen with aging in several NE-rich brain regions, including the hypothalamus, raphe nucleus, and LC, while no age effect is seen on thalamus or red nucleus (Loughlin et al.,1986).

It is unclear whether this decrease in BP_{ND} is due to a decline in the number of neurons or a change in function in those regions. While some postmortem studies have shown a significant loss of LC neurons with aging (Manaye et al., 1995), others using stereological quantification did not replicate this finding (Mouton et al., 1994), although it is possible that structural change occurs without a significant change in LC cell number (e.g., axonal arborization). Although an indirect measure, *in vivo* MRI studies measuring LC signal intensity using the neuromelanin-sensitive MRI technique also had equivocal outcomes, with some studies suggesting age-related changes in subregions of the LC rather than the whole region (Liu et al., 2019; Dahl et al., 2019; Clewett et al., 2016). Additionally, there is an age-related decline in the activation of LC neurons and change in LC functional connectivity (Zhang et al, 2016). These mixed findings suggest the possibility of changes in NE function where [11C]MRB binding could be reduced even without a noticeable decline in neurons or synaptic terminals. This effect might be due to the progressive enveloping of LC terminals with aging (Iwanaga et al., 1996), which might make NET less visible to radioligands. This phenomenon is associated with compensatory downregulation of other molecules involved in the synthesis of NE (Downs et al., 2007), which might lead to a compensatory downregulation of NET itself.

Further investigations on brain NET availability aiming for subjects with wider age ranges would be helpful in understanding age-related changes particularly among older adults. Additionally, age-related declines in NET availability need further investigation regarding the underlying mechanism and the role of NET in older adults in cognitive aging and in the pathophysiology of Alzheimer's disease and related dementias (Peterson and Li,2018).

Consistent with most of the previous findings (with the exception of the thalamus in Li et al., 2014) we did not find differences in BP_{ND} between subjects in the obesity and normal/lean

groups in any regions (supplementary fig. 2/table 1) (Bresch et al., 2017a, Hesse et al., 2017). While this might provide solid evidence of a lack of a relationship, it is important to note that although [11C]MRB is the best available tracer for measuring NET availability, the binding potential values are relatively low and do not have the characteristics of an optimally desirable tracer with higher specific binding. Thus, with low levels of nondisplaceable binding and small regions of interest, there is a higher probability of artifact that may make it challenging to replicate results. In this cohort, the reference region did have a correlation with BMI (0.459, p=0.002) and the time activity curves were lower in obese individuals, which may make the parametric images noisier in this population and therefore more subject to artifact. Relatedly, the Li paper (Li et al., 2014) and the current work have methodigocal differences as the input images are smoothed to different voxel sizes (3 voxels in the current work, 5 voxels in the previous study) and the kinetic modelling rate constant k2' is estimated by MRTM2 currently, while it was a fixed constant previously. These methodical differences between manuscripts do not seem to change the overall BMI results as data processed both ways were similar.

This is the first PET study investigating gender-related differences in NET availability in the healthy human brain. With a relatively even distribution (47% female and 53% male), we did not observe any significant between-group differences in [11C]MRB binding in explored brain regions (supplementary fig. 3). Previously, gender-related differences were found in brown adipose tissue (Hwang et al.,2015), with men having higher [11C]MRB uptake. Also, in a murine study (Mulvey et al.,2018), molecular and functional sex differences in the LC were found, leaving the possibility that there might be anatomic and species-specific sex differences in NE.

Supplementary Material

Refer to Web version on PubMed Central for supplementary material.

Declaration of interest:

The authors report no conflicts of interest with the topic of this work. Marc N. Potenza has consulted for and advised Opiant Pharmaceuticals, Idorsia Pharmaceuticals, Baria-Tek, AXA, Game Day Data and the Addiction Policy Forum; has been involved in a patent application with Yale University and Novartis; has received research support from the Mohegan Sun Casino and Connecticut Council on Problem Gambling; has participated in surveys, mailings or telephone consultations related to drug addiction, impulse control disorders or other health topics; and has consulted for law offices and gambling entities on issues related to impulse control or addictive disorders.

Funding:

This work was supported by the NIH (RL1 AA017540).

References

McMillan PJ, White SS, Franklin A, Greenup JL, Leverenz JB, Raskind MA, & Szot P (2011). Differential response of the central noradrenergic nervous system to the loss of locus coeruleus neurons in Parkinson's disease and Alzheimer's disease. Brain research, 1373, 240–252. [PubMed: 21147074]

Szot P, Leverenz JB, Peskind ER, Kiyasu E, Rohde K, Miller MA, & Raskind MA (2000). Tyrosine hydroxylase and norepinephrine transporter mRNA expression in the locus coeruleus in Alzheimer's disease. Molecular brain research, 84(1-2), 135–140. [PubMed: 11113540]

Kaminski RM, Shippenberg TS, Witkin JM, & Rocha BA (2005). Genetic deletion of the norepinephrine transporter decreases vulnerability to seizures. Neuroscience letters, 382(1-2), 51–55. [PubMed: 15911120]

Klimek V, Stockmeier C, Overholser J, Meltzer HY, Kalka S, Dilley G, & Ordway GA (1997). Reduced levels of norepinephrine transporters in the locus coeruleus in major depression. Journal of Neuroscience, 17(21), 8451–8458. [PubMed: 9334417]

Sigurdardottir HL, Kranz GS, Rami-Mark C, James GM, Vanicek T, Gryglewski G, … & Lanzenberger R (2021). Association of norepinephrine transporter methylation with in vivo NET expression and hyperactivity–impulsivity symptoms in ADHD measured with PET. Molecular psychiatry, 26(3), 1009–1018. [PubMed: 31383926]

Miner LH, Jedema HP, Moore FW, Blakely RD, Grace AA, & Sesack SR (2006). Chronic stress increases the plasmalemmal distribution of the norepinephrine transporter and the coexpression of tyrosine hydroxylase in norepinephrine axons in the prefrontal cortex. Journal of Neuroscience, 26(5), 1571–1578. [PubMed: 16452680]

Weinshenker D, & Schroeder JP (2007). There and back again: a tale of norepinephrine and drug addiction. Neuropsychopharmacology, 32(7), 1433–1451. [PubMed: 17164822]

Ulke C, Rullmann M, Huang J, Luthardt J, Becker GA, Patt M, … & Strauß M (2019). Adult attention-deficit/hyperactivity disorder is associated with reduced norepinephrine transporter availability in right attention networks: a (S, S)-O-[11C] methylreboxetine positron emission tomography study. Translational psychiatry, 9(1), 301. [PubMed: 31732713]

Moriguchi S, Yamada M, Takano H, Nagashima T, Takahata K, Yokokawa K, … & Suhara T (2017). Norepinephrine transporter in major depressive disorder: a PET study. American Journal of Psychiatry, 174(1), 36–41. [PubMed: 27631962]

Ding YS, Lin KS, & Logan J (2006). PET imaging of norepinephrine transporters. Current pharmaceutical design, 12(30), 3831–3845. [PubMed: 17073682]

Ding YS, Lin KS, Logan J, Benveniste H, & Carter P (2005). Comparative evaluation of positron emission tomography radiotracers for imaging the norepinephrine transporter:(S, S) and (R, R) enantiomers of reboxetine analogs ([11C] methylreboxetine, 3-Cl-[11C] methylreboxetine and [18F] fluororeboxetine),(R)-[11C] nisoxetine,[11C] oxaprotiline and [11C] lortalamine. Journal of neurochemistry, 94(2), 337–351. [PubMed: 15998285]

Lorang D, Amara SG, & Simerly RB (1994). Cell-type-specific expression of catecholamine transporters in the rat brain. Journal of Neuroscience, 14(8), 4903–4914. [PubMed: 8046459]

Manaye KF, McIntire DD, Mann DM, & German DC (1995). Locus coeruleus cell loss in the aging human brain: A non-random process. Journal of Comparative Neurology, 358(1), 79–87. [PubMed: 7560278]

Chan-Palay V, & Asan E (1989). Quantitation of catecholamine neurons in the locus coeruleus in human brains of normal young and older adults and in depression. Journal of Comparative Neurology, 287(3), 357–372. [PubMed: 2570793]

Vijayashankar N, & Brody H (1979). A quantitative study of the pigmented neurons in the nuclei locus coeruleus and subcoeruleus in man as related to aging. Journal of Neuropathology & Experimental Neurology, 38(5), 490–497. [PubMed: 469568]

Ding YS, Singhal T, Planeta-Wilson B, Gallezot JD, Nabulsi N, Labaree D, … & Malison RT (2010). PET imaging of the effects of age and cocaine on the norepinephrine transporter in the human brain using (S, S)-[11C] O-methylreboxetine and HRRT. Synapse, 64(1), 30–38. [PubMed: 19728366]

Shang Y, & Dluzen DE (2002). Castration increases nisoxetine-evoked norepinephrine levels in vivo within the olfactory bulb of male rats. Neuroscience letters, 328(2), 81–84. [PubMed: 12133560]

Yang SP, Francis Pau KY, & Spies HG (1997). Gonadectomy alters tyrosine hydroxylase and norepinephrine transporter mRNA levels in the locus coeruleus in rabbits. Journal of neuroendocrinology, 9(10), 763–768. [PubMed: 9355045]

Chiang-shan RL, Potenza MN, Lee DE, Planeta B, Gallezot JD, Labaree D, … & Neumeister A (2014). Decreased norepinephrine transporter availability in obesity: positron emission tomography imaging with (S, S)-[11C] O-methylreboxetine. Neuroimage, 86, 306–310. [PubMed: 24121204]

Hesse S, Becker GA, Rullmann M, Bresch A, Luthardt J, Hankir MK, … & Sabri O (2017). Central noradrenaline transporter availability in highly obese, non-depressed individuals. European journal of nuclear medicine and molecular imaging, 44(6), 1056–1064. [PubMed: 28066877]

Bresch A, Rullmann M, Luthardt J, Becker GA, Reissig G, Patt M, … & Hesse S (2017). Emotional eating and in vivo norepinephrine transporter availability in obesity: a [11C] MRB PET pilot study. International Journal of Eating Disorders, 50(2), 152–156. [PubMed: 27611116]

Bresch A, Rullmann M, Luthardt J, Becker GA, Patt M, Ding YS, … & Hesse S (2017). Hunger and disinhibition but not cognitive restraint are associated with central norepinephrine transporter availability. Appetite, 117, 270–274. [PubMed: 28647385]

Vettermann FJ, Rullmann M, Becker GA, Luthardt J, Zientek F, Patt M, … & Hesse S (2018). Noradrenaline transporter availability on [11C] MRB PET predicts weight loss success in highly obese adults. European Journal of Nuclear Medicine and Molecular Imaging, 45(9), 1618–1625. [PubMed: 29627935]

Hannestad J, Gallezot JD, Planeta-Wilson B, Lin SF, Williams WA, van Dyck CH, … & Ding YS (2010). Clinically relevant doses of methylphenidate significantly occupy norepinephrine transporters in humans in vivo. Biological psychiatry, 68(9), 854–860. [PubMed: 20691429]

Ichise M, Liow JS, Lu JQ, Takano A, Model K, Toyama H, … & Carson RE (2003). Linearized reference tissue parametric imaging methods: application to [11C] DASB positron emission tomography studies of the serotonin transporter in human brain. Journal of Cerebral Blood Flow & Metabolism, 23(9), 1096–1112. [PubMed: 12973026]

Ding YS, Lin KS, Garza V, Carter P, Alexoff D, Logan J, … & King P (2003). Evaluation of a new norepinephrine transporter PET ligand in baboons, both in brain and peripheral organs. Synapse, 50(4), 345–352. [PubMed: 14556239]

Carson RE, Barker WC, Liow JS, & Johnson CA (2003, October). Design of a motion-compensation OSEM list-mode algorithm for resolution-recovery reconstruction for the HRRT. In 2003 IEEE Nuclear Science Symposium. Conference Record (IEEE Cat. No. 03CH37515) (Vol. 5, pp. 3281–3285). IEEE.

Tzourio-Mazoyer N, Landeau B, Papathanassiou D, Crivello F, Etard O, Delcroix N, … & Joliot M (2002). Automated anatomical labeling of activations in SPM using a macroscopic anatomical parcellation of the MNI MRI single-subject brain. Neuroimage, 15(1), 273–289. [PubMed: 11771995]

Loughlin SE, Foote SL, & Bloom FE (1986). Efferent projections of nucleus locus coeruleus: topographic organization of cells of origin demonstrated by three-dimensional reconstruction. Neuroscience, 18(2), 291–306. [PubMed: 3736860]

Manaye KF, McIntire DD, Mann DM, & German DC (1995). Locus coeruleus cell loss in the aging human brain: A non-random process. Journal of Comparative Neurology, 358(1), 79–87. [PubMed: 7560278]

Mouton PR, Pakkenberg B, Gundersen HJG, & Price DL (1994). Absolute number and size of pigmented locus coeruleus neurons in young and aged individuals. Journal of chemical neuroanatomy, 7(3), 185–190. [PubMed: 7848573]

Liu KY, Acosta-Cabronero J, Cardenas-Blanco A, Loane C, Berry AJ, Betts MJ, … & Hämmerer D (2019). In vivo visualization of age-related differences in the locus coeruleus. Neurobiology of aging, 74, 101–111. [PubMed: 30447418]

Dahl MJ, Mather M, Düzel S, Bodammer NC, Lindenberger U, Kühn S, & Werkle-Bergner M (2019). Rostral locus coeruleus integrity is associated with better memory performance in older adults. Nature Human Behaviour, 3(11), 1203–1214.

Clewett DV, Lee TH, Greening S, Ponzio A, Margalit E, & Mather M (2016). Neuromelanin marks the spot: identifying a locus coeruleus biomarker of cognitive reserve in healthy aging. Neurobiology of aging, 37, 117–126. [PubMed: 26521135]

Zhang S, Hu S, Chao HH, & Li CSR (2016). Resting-state functional connectivity of the locus coeruleus in humans: in comparison with the ventral tegmental area/substantia nigra pars compacta and the effects of age. Cerebral Cortex, 26(8), 3413–3427. [PubMed: 26223261]

Iwanaga K, Yamada M, Wakabayashi K, Ikuta F, & Takahashi H (1996). A newly discovered age-related synaptic change in the human locus ceruleus: morphometric and ultrastructural studies. Acta neuropathologica, 91(4), 337–342. [PubMed: 8928609]

Downs JL, Dunn MR, Borok E, Shanabrough M, Horvath TL, Kohama SG, & Urbanski HF (2007). Orexin neuronal changes in the locus coeruleus of the aging rhesus macaque. Neurobiology of aging, 28(8), 1286–1295. [PubMed: 16870307]

Peterson AC, & Li CSR (2018). Noradrenergic dysfunction in Alzheimer's and Parkinson's diseases—An overview of imaging studies. Frontiers in Aging Neuroscience, 10, 127. [PubMed: 29765316]

Hwang JJ, Yeckel CW, Gallezot JD, Belfort-De Aguiar R, Ersahin D, Gao H, … & Ding YS (2015). Imaging human brown adipose tissue under room temperature conditions with 11C-MRB, a selective norepinephrine transporter PET ligand. Metabolism, 64(6), 747–755. [PubMed: 25798999]

Mulvey B, Bhatti DL, Gyawali S, Lake AM, Kriaucionis S, Ford CP, … & Dougherty JD (2018). Molecular and functional sex differences of noradrenergic neurons in the mouse locus coeruleus. Cell reports, 23(8), 2225–2235. [PubMed: 29791834]

Mather M, & Harley CW (2016). The locus coeruleus: essential for maintaining cognitive function and the aging brain. Trends in cognitive sciences, 20(3), 214–226. [PubMed: 26895736]

Shibata E, Sasaki M, Tohyama K, Kanbara Y, Otsuka K, Ehara S, & Sakai A (2006). Age-related changes in locus ceruleus on neuromelanin magnetic resonance imaging at 3 Tesla. Magnetic Resonance in Medical Sciences, 5(4), 197–200. [PubMed: 17332710]

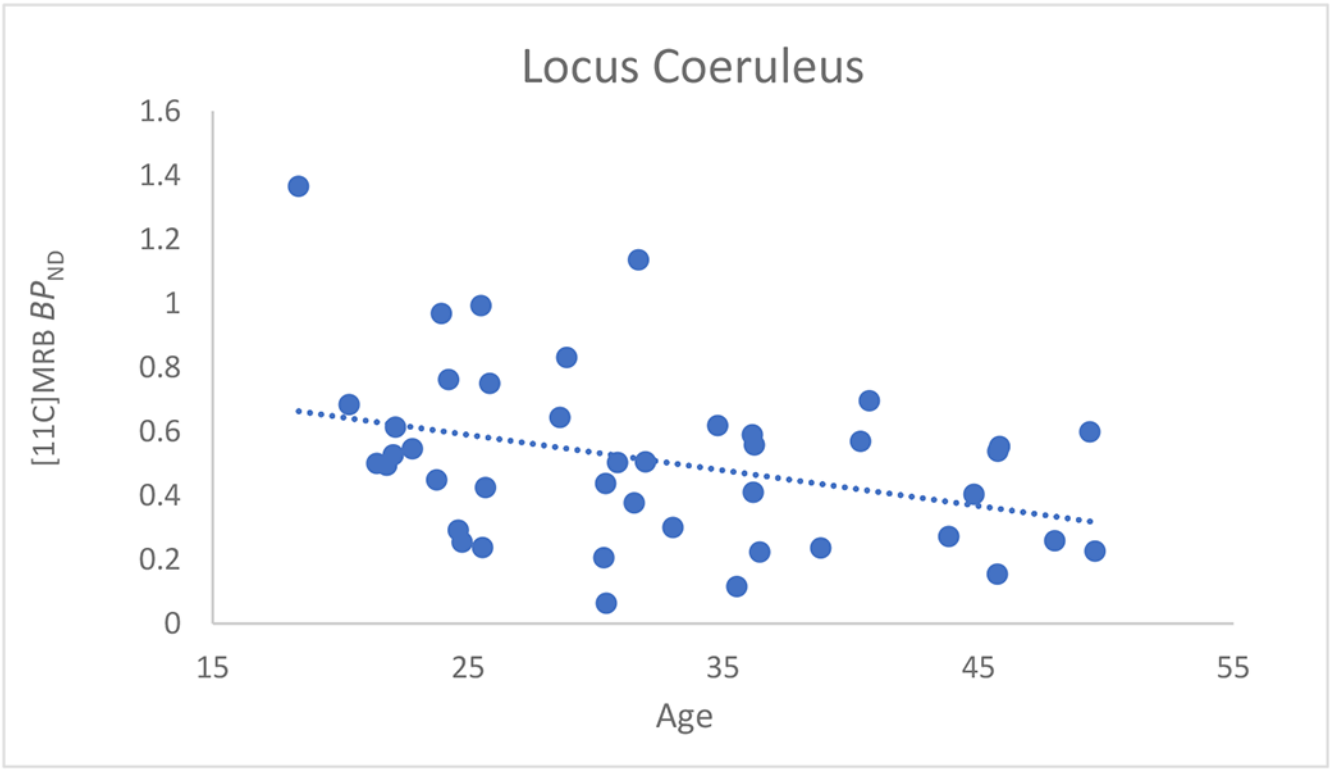

FIGURE 1.

Scatterplot of BP_{ND} versus age (in years) in the locus coeruleus. The dashed line shows the Pearson correlation: R= −0.36, P<0.01

TABLE 1.

Mean values, slope between age and regional [11C]MRB BP_{ND}. Correlations with age and BP_{ND} and average decreases per decade are shown. The Pr (>|t|) column represents the p-value associated with the t value.

Region	BP_{ND}		Slope		Pr > |t|	Pearson R	Decrease per decade
	Mean	SD	Estimate	Standard Error			
Hypothalamus	**0.6169**	**0.2903**	**−0.01234**	**0.004962**	**0.0174**	−0.3	−14%
Locus coeruleus	**0.5082**	**0.2701**	**−0.01329**	**0.004399**	**0.0045**	−0.36	−17%
Red nucleus	0.4765	0.2656	−0.00594	0.004799	0.2232	−0.12	−7%
Pulvinar	0.5416	0.2252	−0.0059	0.003962	0.1448	−0.14	−6%
Raphe nucleus	**0.671**	**0.3246**	**−0.01923**	**0.004996**	**0.0004**	−0.46	−19%
Thalamus	0.4934	0.1721	−0.00498	0.003114	0.1181	−0.14	−5%